Abstract # 1104

Identification of effective treatment regimens for ovarian cancer using tumor histoculture platform

Biswajit Das[1], Kowshik Jaganathan[1], Rohit Ranade[2], C Jayaprakash[3], Ravi Krishnappa[4], Syamkumar V[1], Chandan Bhowal[1], Mouniss M[1], Dharanidharan M[1], Rajashekar M[1], Oliyarasi M[1], Ritu Malhotra[1], Govindraj K[1], Nandini Pal Basak[1, #], Satish Sankaran[1, *]

[1]Farcast Biosciences Pvt Ltd, India; [2]Mazumdar Shaw Medical Centre, Bangalore; [3]DBR & SK Superspeciality Hospital, Tirupati; [4]JSS hospital, Mysore

[#]Presenting author, *corresponding author.

Background

The prognosis of ovarian cancer (OvCa) is poor, with a 5-year survival rate in patients of 59.60% (95% CI, 56.06-63.13) [1]. Personalized treatment regimens could improve treatment outcome and quality of life. We developed the Farcast™ TruTumor Ovarian Cancer histoculture platform to predict response to therapies enabling personalized treatment options for every patient.

Methods

Patient tissue samples: Freshly resected ovarian cancer (OvCa) tissue sample along with matched blood (n=10) were collected from consented patients.

Histo-Culture workflow: Tissue was processed to generate explants, and were distributed into arms and cultured for 72 h. The functional fidelity of immune components was assessed by stimulating these with anti-CD3 (0.01 µg/ml) + Interleukin-2 (IL2, 100 µg/ml), or with Lipopolysaccharides (LPS, 1 µg/ml). Tumor cytotoxicity to treatment was evaluated with Platin (Cisplatin:3.3 µg/ml, or Carboplatin: 37.1 µg/ml) and/or Taxane (Docetaxel:2 µg/ml, or Paclitaxel:2.7 µg/ml), or Nivolumab (132 µg/ml). Fresh media was replaced every 24 h and the collected supernatant was used for cytokine analysis

Flow cytometry analysis: Post treatment the explants were dissociated into single cells and stained with with Live/Dead dye, surface antibodies and intracellular antibodies. Data was acquired in BD LSR Fortessa and analysed using FlowJo.

Cytokine Analysis: The supernatants collected were used for analysis of cytokine released with Procarta 5 Plex kit. Data was analysed using Milliplex analyst software.

H&E & IHC: H&E and cleaved caspase 3 IHC was performed with 4µm FFPE sections using Leica automated multi-stainer system and Ventana IHC automated staining system respectively. Scoring was performed by certified pathologist for tumor content, immune content and infiltrating immune cells (% immune cell proximal to tumor nest). Cleaved caspase 3 staining was evaluated in the tumor compartment.

Statistical analysis: All data analysis and graphical representations were done using GraphPad Prism (Version 9). Wilcoxon matched-pairs signed rank t-test for paired data and Mann-Whitney t-test for unpaired data, was used to generate P-values. P value significance is represented as * (p<0.05) ** (p<0.01).

Patient demography

Parameters	Category	Number (%)
Age	<48	5 (50%)
	≥48	5 (50%)
Grade	Low grade	2 (20%)
	High grade	8 (80%)
Stage	I	1 (10%)
	III	6 (60%)
	Unknown	3 (30%)
Primary/Metastatic	Primary	9 (90%)
	Metastatic	1 (10%)
Prior treatment given	Yes	7 (70%)
	No	3 (30%)
Tumor Site	Ovary	9 (90%)
	Omentum	1 (10%)

Table 1: Demography of patient (n=10) sample used for histoculture and chemosensitivity.

Farcast[tm] TruTumor histoculture platform

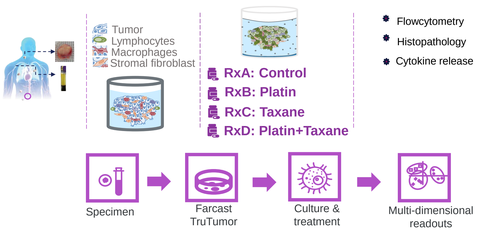

Fig 1: Schematic representation of experimental design and workflow during treatment.

Baseline immune content in OvCa was lower in comparison to Head and Neck cancer but similar to Renal Cell Carcinoma

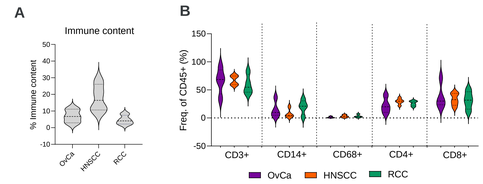

Fig 2: Violin plot representing the distribution of immune content in ovarian cancer (OvCa), head and neck squamous cell carcinoma (HNSCC), and renal cell carcinoma (RCC) **A**. Immune content **B.** Immune subtypes at baseline.

OvCa samples exhibited a higher proportion of lymphocytes

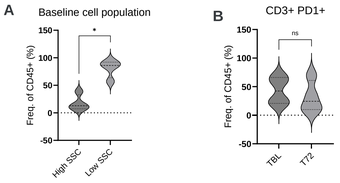

Fig 3: Violin plot representing the distribution of **A**. High SSC and Low SSC immune cell population at baseline **B.** population of CD3+ PD1+ immune cells at baseline and post culture in OvCa (n=4).

Histological morphology of tumor and stroma preserved during culture

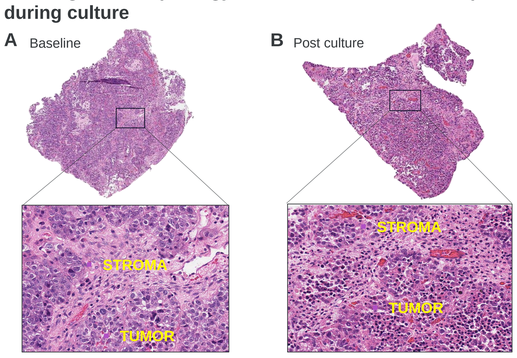

Fig 4: Representative images of H&E-stained sections of **A**. Baseline **B.** Post-culture OvCa samples.

Immune cell sub-populations are preserved post culture

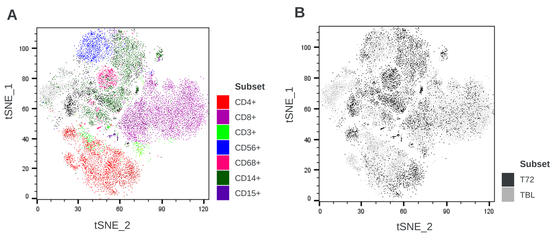

Fig 5: **A.** Immune subpopulation represented as tSNE plot **B.** distribution of immune population at baseline and post culture in OvCa samples (n=4)

Increase in T-cell activity and proliferation observed on anti-CD3+IL2 stimulation

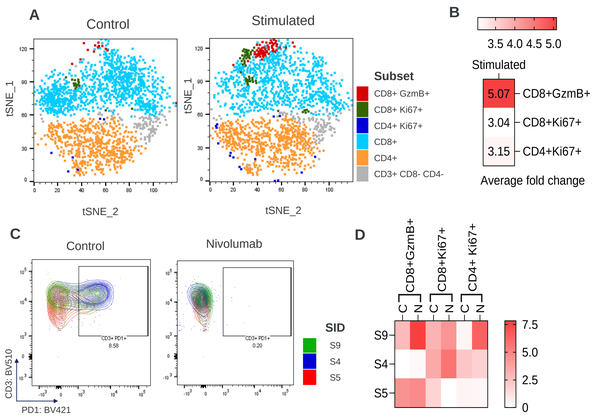

Fig 6: **A.** tSNE plot on CD3+ population from control and anti-CD3+IL2 stimulated samples, (n=3) **B.** heatmap representing fold change in immune subpopulation upon stimulation **C.** contour plot of control and Nivolumab treated samples (n=3). **D.** Heatmap representing changes in immune subpopulation as percentage of parents upon Nivolumab (N) treatment.

T cell and myeloid cell specific response observed with Anti-CD3/IL2 and LPS stimulation respectively

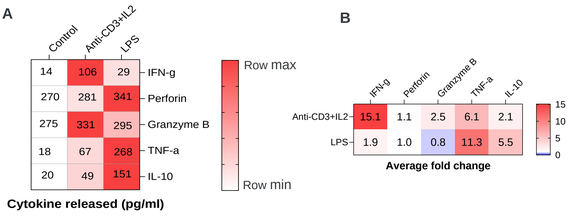

Fig 7: **A.** Heatmap of cytokine released (pg/ml) upon stimulation with anti-CD3+IL2 or LPS. **B.** Heatmap of cytokine released upon stimulation as a function of averaged fold change (n=3) after T0 normalization

Heterogeneous response to chemotherapy treatment observed across patient samples

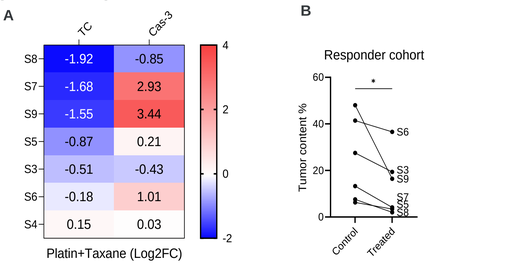

Fig 8: **A.** Heatmap of change in tumor content (TC) and cleaved caspase 3 (Cas-3) upon Platin+Taxane treatment with respect to untreated control as a function of Log2FC (n=7)
B. Graphical representation of tumor content in control and treated arm.

Clinical correlation of chemotherapy response in OvCa samples

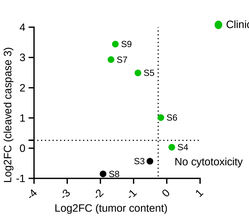

TruTumor response

Clinical response	Responder	Non Responder
Responder	4	
Non responder		1

Fig 9: A. Two-dimensional dot plot representation of Log2 fold change of tumor content and cleaved caspase 3 expression in tumor evaluated using TruTumor platform. **B.** Concordance between TruTumor and clinical response.

Conclusions

The Farcast™ OvCa TruTumor platform facilitates simultaneous investigation with multiple drug treatment regimens to select the optimal therapy option, enabling personalized treatment decision making for patients.

References

Maleki, Z., et al. (2023), BMC Cancer, 23(1), 558.